water

MDPI

Article

Experimental Investigation of Leakage Flow Rate and Fluidisation beneath Polyethylene Pipes in Non-Uniform Soils

Shahab Sharafodin [1], Milad Latifi [2,*] and Masoud Ghodsian [1]

[1] Faculty of Civil and Environmental Engineering, Tarbiat Modares University, Tehran P.O. Box 14115-143, Iran; s_sharafodin@modares.ac.ir (S.S.); ghods@modares.ac.ir (M.G.)
[2] Centre for Water Systems, Faculty of Environment, Science and Economy, University of Exeter, Exeter EX4 4QF, UK
* Correspondence: m.latifi@exeter.ac.uk

Abstract: Soil fluidisation around buried pipes is one of the water leakage effects that has a direct influence on the ultimate failure of pipelines. In this research, using a laboratory model, the fluidisation caused by water leakage from three cracks with three lengths (14, 17, and 20 mm) and a 3 mm diameter hole for five pressures (1.5–5.5 bar) in non-uniform soils has been evaluated. The experiments were carried out both for pipes buried in soil, as well as exposed pipes. In the buried pipe tests, leakage flow rate, fluidisation, and mobile bed zone dimensions were investigated. The results showed that the increase in leakage flow rate due to an increase in pressure and crack length in exposed pipes is higher than in buried pipes. The exponent of the leakage–pressure relationship was obtained between 0.40 and 0.47 for the hole and between 0.8 and 1.9 in the crack. Observing different development patterns for fluidisation and mobile bed zones in cracks and holes, new relationships are presented for the height, width, and cross-sectional area of the leakage zones.

Keywords: water leakage from cracks; soil fluidisation; mobile bed; pipe failure; water distribution networks

Citation: Sharafodin, S.; Latifi, M.; Ghodsian, M. Experimental Investigation of Leakage Flow Rate and Fluidisation beneath Polyethylene Pipes in Non-Uniform Soils. *Water* **2024**, *16*, 1156. https://doi.org/10.3390/w16081156

Academic Editor: Marco Franchini

Received: 17 March 2024
Revised: 10 April 2024
Accepted: 17 April 2024
Published: 19 April 2024

1. Introduction

Water distribution systems worldwide are ageing and failing, while the demand for these systems, and hence natural water supplies, is growing. Losses in water distribution systems are at alarmingly high levels in many towns and cities worldwide. Physical losses (leaks), illicit usage, non-metered consumption, and under-registration of water meters are all examples of water losses. Leakage accounts for a significant portion of overall water losses, sometimes exceeding 70% [1]. In developing countries, roughly 45 million cubic meters of water are lost daily, with an economic value of over USD 3 billion annually [2]. With a per capita usage of 150 litres per day, the savings from only a one-third reduction in non-revenue water (NRW) production could provide water for 800 million people. In addition, reducing NRW can lead to improved reliability of water services, enhanced access to clean water for urban poor communities, higher water quality, reduced energy consumption, and, in certain cases, a delay in the need for expanding water supply infrastructure [3].

Water distribution pipes have different states and patterns of damage. Mora-Rodrigues et al. [4] classified pipe failures into three categories: (1) circumferential breaks, caused by longitudinal tension; (2) longitudinal breaks, caused by cross-sectional tension (radial tension); and (3) cracks in unions resulting from cross-sectional tension in the pipe union. In the case of internally pressurised pipes, the theoretical circumferential stress is twice as high as the longitudinal stress [5], thereby leading to a greater occurrence of longitudinal cracks due to internal pressure loads.

Pressure is one of the most critical factors that impact leakage from distribution systems. The orifice flow equation demonstrates that leakage from water distribution

systems is relatively insensitive to pressure, changing in proportion to the square root of pressure [6]:

$$Q = C_d A \sqrt{2gh}. \quad (1)$$

Q is the flow rate, C_d is the discharge coefficient, A is the orifice cross-sectional area, g is gravity acceleration, and h is the pressure head differential over the orifice. Although Equation (1) correctly highlights the evident dependency of leakage on water pressure, it is unreliable in describing experimental data obtained from field research and laboratory experiments concerning specific pipe materials [7].

Equation (2) is the basis of the leakage–pressure equation proposed by the International Water Association (IWA) water loss task force [8]:

$$Q = C\ P^N. \quad (2)$$

C is the leakage coefficient; P is the pressure inside the pipe; and N is the leakage exponent. The relationship between pressure and leakage is not a new concept, and its power-law form has been shown in previous studies. Various studies have shown that leakage in water distribution systems frequently varies with pressure, exhibiting a leakage exponent higher than the theoretical orifice value of 0.5 [9,10].

Farley and Trow [11] found that the average leakage exponent is approximately 1.15, but values as low as 0.5 and as high as 2.79 have been observed. van Zyl and Clayton [1] assumed that the pressure–leakage relationship is influenced by four parameters, which include pipe material behaviour, resulting in an extension of the leak area with increased pressure, leak hydraulics, soil hydraulics, and water demand.

Greyvenstein and van Zyl [10] investigated different pipe materials, including asbestos cement, steel, and uPVC, as well as types of leakage, such as circular orifice, circumferential crack, longitudinal crack, and corrosion, to analyse their effects on leakage power. Based on their observations, they concluded that steel pipes exhibit the highest leakage due to corrosion. However, other investigations indicate that the leakage exponent of longitudinal slits in HDPE pipes is more significant compared to other pipe materials, as noted by Sadr-Al-Sadati and Ghazizadeh [12]. Zhai et al. [13] introduced a new equation to estimate the hydraulic conductivity of unsaturated soil, taking into consideration the effects of film flow.

Latifi et al. [14] demonstrated a strong correlation between leakage and specific factors, namely grain diameter over 50% passage, plastic limit, and hydraulic permeability. In a subsequent study, Latifi et al. [15] conducted experimental investigations on pipe leakage with various soil compositions. Their findings indicate that soil properties are more accurately represented by the particle diameter at 50% passing (D_{50}), dry unit weight (γ_d), and hydraulic permeability coefficient (k). Furthermore, no significant correlation was observed between soil properties and leakage.

Fluidisation

Recent studies have found that if a high flow rate is present, a leak in a water distribution pipe can internally fluidise the soil just around the leak [6]. This fluidisation is defined as the transformation of a granular media into a fluid-like condition [16]. When inter-particle forces reduce and particles are free to move with the pore fluid (i.e., the particles become separated and in motion), fluidisation of a granular material occurs (Figure 1). In an upward flow, the area where the water and soil particles flow upward and finally rotate is called the fluidised zone, and the surrounding zone, where the water and particles flow downward, is called the mobile bed zone [17].

A limited number of research studies have been conducted to examine the impact of leakage on soil parameters. Van Zyl et al. [6] experimentally modelled a leak in glass ballotini beads, with the flow direction being vertically upward. According to the study, the orifice and the two inner zones (fluidised and mobile bed) are where the bulk of the mechanical energy is lost in the leaky jet. The study also showed that significant pressures

could be maintained inside the pipe without the fluidised zone reaching the surface of the glass beads' bed. Alsaydalani and Clayton [16] stated that when the upward seepage force equals the buoyant weight of the preceding granular bed, the granular soil moves away from the opening. It was also discovered that the flow velocity, particle size and sphericity, bed height, and permeability are the main factors that affect the seepage force, which governs the start of internal fluidisation. Bailey and van Zyl [18] conducted experimental investigations and found that the pore pressure in the bed reaches its maximum value above the fluidisation zone. However, beyond the fluidisation zone, the pressure sharply decreases. Additionally, it has been observed that at a height above 1 m from the pipe, the pressure decreases linearly with the increase in height.

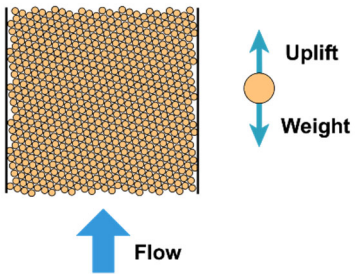

Figure 1. Schematic diagram of the fluidisation condition in a porous media [6].

Pike et al. [19] carried out a laboratory study on the failure of the upper pipe surface caused by fluidisation resulting from leakage. They discovered substantial erosion of the pipe material, leading to the formation of new leak holes in the surface. Scouring gradually increased the volume, depth, length, and width of the affected area. The failure rate was primarily influenced by the direction of the leakage jet, followed by the leakage flow, size of the sand particles, pipe material, and coating depth. Latifi et al. [17] conducted an experiment using a box containing a uPVC pipe with a longitudinal crack on the crown. The pipe was buried under various types of soil, and water was then pushed through it. The findings revealed a strong correlation between water pressure and the maximum height and area of the zones. The hydraulic critical state is significantly influenced by soil porosity and uniformity coefficient. Specifically, higher porosity results in a smaller magnitude of the critical hydraulic gradient [20]. Particle size, particle shape, bed height, and defect breadth affect soil bedding leaks and fluidisation. High-spherical materials, coarser soil particles, and a greater bed height fluidised at higher leakage rates and pressure [21]. Soil porosity plays a crucial role in soil fluidisation, and reducing soil porosity can enhance the stability of the soil bed [22]. Akrami et al. [23] noted that as the flow rate and porosity of the sand sample increased, it marked the beginning of soil deformation. During fluidisation, tests with higher relative density (RD) and finer sand samples exhibited considerably greater extents of failure.

Developing the fluidisation zone around leak points in a water pipe leads to soil washout, losing the bearing capacity of the soil, and eventual failure of the pipe, resulting in significant expenditures for maintenance purposes [24]. As water jets out from the pipe's leak, it washes away the nearby soil, specifically removing the fine particles due to their light weight. This results in alterations in the soil's characteristics such as grading, porosity, and hydraulic permeability. With the fine particles being carried off, the soil loses its cohesion, becoming loose and decreasing its capacity to support the pipe. Consequently, this situation may lead to the pipe either breaking or its joint dismantling. Therefore, investigating this phenomenon has garnered attention in recent years. This study focuses on investigating the leakage flow rate and fluidisation dimensions of three longitudinal cracks and one circular orifice. The primary objectives of this experimental study are to explore (1) leakage flow rate and fluidisation in non-uniform soil; (2) the impact of crack length on leakage flow rate and fluidisation; and (3) the differences in leakage flow rate and fluidisation between cracks and orifices. Additionally, unlike the majority of earlier studies

that primarily examined failures occurring on top of the pipe, this research examines a different scenario where the leak is located at the pipe's invert. The results of this research will assist engineers in estimating the extent of the fluidised zone around the pipe, thereby aiding in the prevention of pipe failures due to soil scouring.

2. Materials and Methods

In this study, a laboratory set-up was used to explore the effects of crack size and shape on pipe leakage. The investigation considered a constant pipe material, orifice, and leak opening. The set-up comprised a water storage tank, a centrifugal pump, regulating valves, metal pipe connections, a polyethylene pipe, an analogue pressure gauge, and a soil box. The leaky pipe was positioned adjacent to the glass wall of the box, enabling observation of fluidisation and mobile bed zones. It should be noted that the glass wall permits only half of the fluidisation and mobile bed zones to develop. Moreover, the boundary condition effects of the glass wall may result in the formation of smaller zones around the pipe. Experiments were carried out to measure the leakage flow rate and dimensions of the fluidisation zone in the surrounding soil from different sizes of cracks and holes. The pressure inside the pipe was increased in steps of 1 bar, starting from 1.5 bar and reaching 5.5 bar. The adjustment of the pressure was controlled using the regulating valve. In each test, pressure was applied inside the pipe to form a leakage jet from the hole/crack. Leakage flow was measured based on the water drained from the bottom of the box. Also, the dimensions of the fluidisation zone and mobile bed zone were measured through the glass wall of the box. Figure 2 shows the schematics of the experimental set-up used in this research.

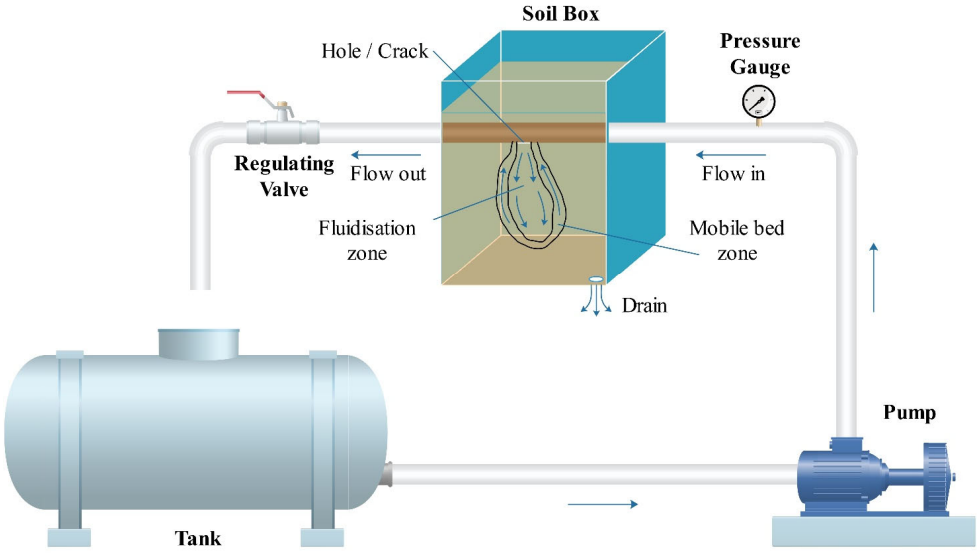

Figure 2. Schematic view of the experimental set-up.

Since in most design standards of water distribution networks, the maximum allowable pressure is 6 bar, in this study, the internal pressures were set in the range of 1.5–5.5 bar. Steel pipes connect the set-up components to a 40 mm polyethylene pipe that passes through the soil box. Another pipe was used to return the water flow to the storage tank, forming a closed loop. The soil box had dimensions of 1000 × 800 × 1000 mm with an open top. A calibrated analogue pressure gauge with an accuracy of ±0.1 bar was utilized at the discharge of the centrifugal pump to measure pressure values.

Polyethylene pipes, one of the most widely used materials in urban water distribution networks, were applied to simulate field conditions in city environments. A PE80 PN10 pipe with a 40 mm outer diameter and a 36 mm inner diameter was deployed. In order to drain and quantify the leaked water, a 50 mm diameter orifice was used at the bottom of the box. In each test, the drained water from the box was weighed using a scale with a

precision of 1 g, equal to 0.001 L, while the draining time was measured with a stopwatch accurate to 0.01 s in 10 min steps. All data were reported once steady-state conditions were confirmed throughout the study. The flow rate was calculated by dividing the measured volume of water by the recorded time.

Given the prevalent availability of non-uniform soils in natural settings, the utilisation of such soil types in this study aimed to enhance the accuracy of modelling the pipe's surrounding environment. For sand, when the uniformity coefficient ($C_u = D_{60}/D_{10}$) is equal to or greater than 6, the soil is classified as non-uniform [25]. In order to simulate non-uniform soil, seven types of uniform soils with different gradations were used, and two non-uniform soils were formed by mixing uniform soils in a specific ratio, each of which had an average size (D_{50}) of 1.27 and 1.17 mm and a C_u of 7.7 and 6.0, respectively. Characteristics of soils #1 and #2 are presented in Table 1, and the gradation curve (resulting from the sieve test) for both soils is demonstrated in Figure 3. It can be seen that even though Soil #1 and Soil #2 have similar fine-grain characteristics, they differ significantly when it comes to coarse-grain properties. Specifically, Soil #1 has a D_{80} value of 3.97, while Soil #2 has a D_{80} value of 2.19. It should be mentioned that Soil #1 had coarser grains and Soil #2 had finer grains. Soil #1 was classified as SP, which stands for poorly graded sand, while Soil #2 was categorized as SW, which represents well-graded sand, based on the specifications outlined in [26]. The soil was compacted using a proctor hammer with 70 blows for each 15 cm layer in all tests. This is essential for ensuring consistency and facilitating the comparison of test results. Moreover, in order to obtain the optimal soil moisture content, the standard compaction test [27] was done for both soil samples. The value of 11.5% for Soil #1 and 14.5% for Soil #2 was determined as the optimal soil moisture content, and this amount of water was added to dry soils before pouring into the box to guarantee maximum compaction. Prior to each test, water was added to fully saturate the soil, guaranteeing that all the soil pores were occupied and causing water to flow out from the drain located at the base of the box. Fluidising the soil during the tests made it loose, so fresh soil was employed for each new test run to prevent the effect of one test on the next.

Table 1. Properties of soils used in this research.

Soil	D_{10} (mm)	D_{30} (mm)	D_{50} (mm)	D_{60} (mm)	$C_u = D_{60}/D_{10}$	C_c	ω_{opt} (%)	γ_d (kN/m^3)	n	Classification
Soil #1	0.3	0.52	1.27	2.30	7.7	0.39	11.5	16.72	0.35	SP
Soil #2	0.26	0.61	1.17	1.55	6.0	1.05	14.5	18.53	0.28	SW

Notes: C_u: coefficient of uniformity; C_c: coefficient of curvature; ω_{opt}: optimum moisture; γ_d: dry density at maximum density; and n: porosity.

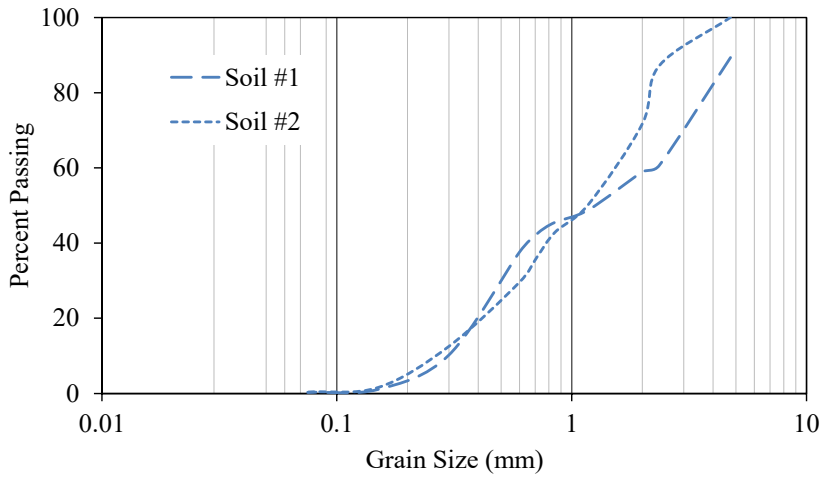

Figure 3. Gradation curve of soils used in this research.

To investigate the effect of crack size and shape on the leakage flow rate and soil fluidisation, four different failures were simulated. These included three cracks with

lengths of 14, 17, and 20 mm and a hole with a diameter of 3 mm, all deliberately created in the polyethylene pipe. (Figure 4). These crack lengths were selected because the 14 mm crack was the smallest to form fluidisation and mobile bed zones under the range of pressures in this research, and the 20 mm crack was the largest to fit within the height of the fluidisation and mobile bed zones in the box. The pipe was positioned within the box so that the crack or hole ejects water parallel to the glass wall and perpendicular to the bottom of the box. This is crucial to maintain consistency and enable the comparison of test results.

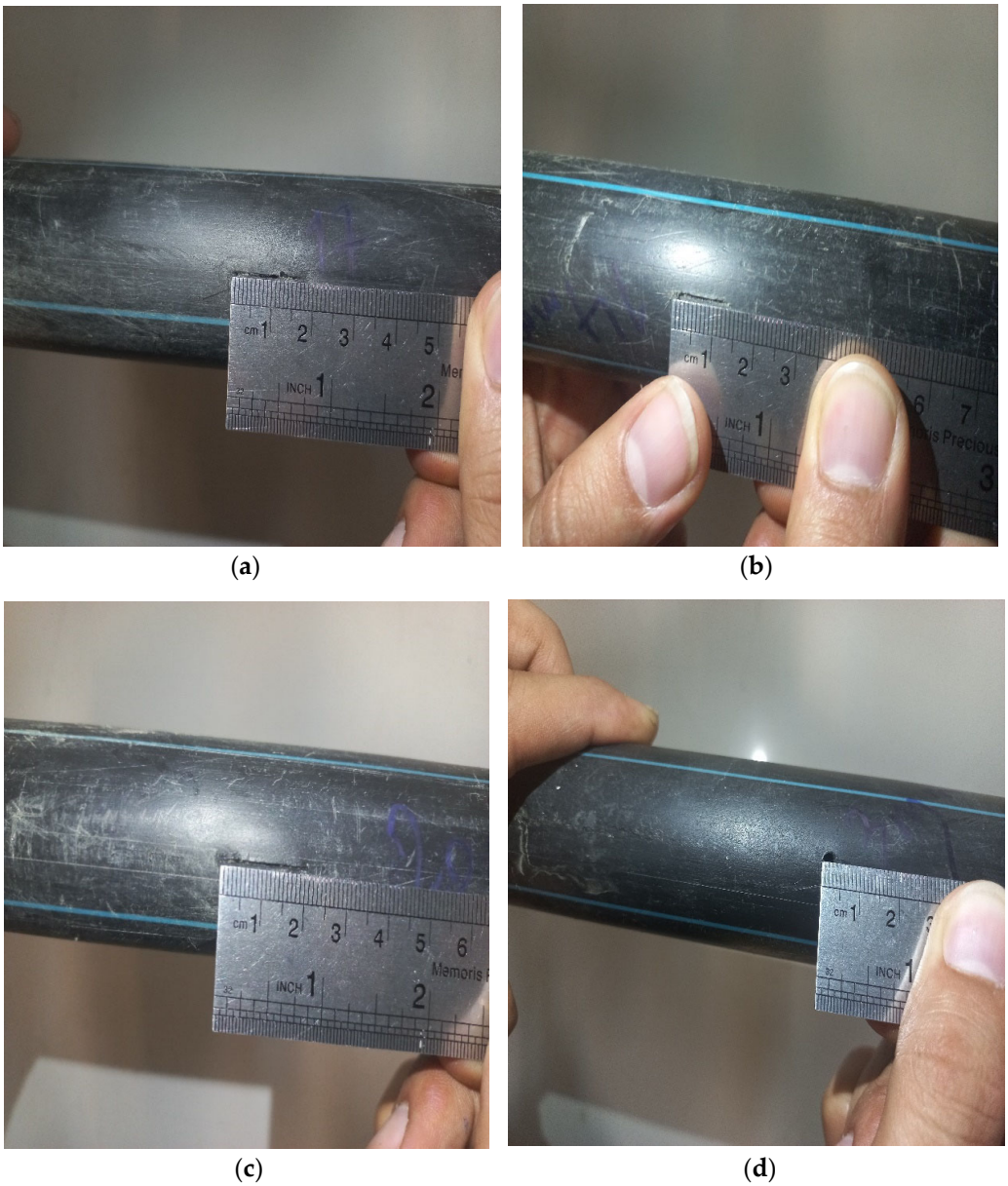

Figure 4. Various failures created on the pipes: (**a**) 14 mm crack, (**b**) 17 mm crack, (**c**) 20 mm crack, and (**d**) 3 mm hole.

To keep it concise, the mentioned leaks were named Crack-14, Crack-17, Crack-20, and Hole-3, respectively. Two sets of failure shapes were created to have different geometries but with nearly the same leak area. For instance, Crack-14 had a rectangular leak size of 14 × 0.5 mm, with an area (A_0 = 7 mm^2) that was approximately equal to that of Hole-3. The development of fluidisation and mobile bed zones was recorded using a camera positioned in front of the glass wall.

3. Results and Discussion

This section focuses on analysing the results and finding correlations to study the effects of the shape and size of failures on leakage discharge and fluidisation zone dimensions. Several experiments were carried out, consisting of four types of failures and two non-uniform soils under five pressures between 1.5 and 5.5 bar. The mentioned pressures are based on the pressure inside the pipe. Figure 5 depicts the variations in leakage pressure for three cases: leakage to air, leakage to two types of soil, and four different failure shapes. This figure shows that, in all cases, the leakage increases by increasing the pressure. Moreover, in each experiment, the highest amount of leakage occurs in the absence of the soils (i.e., leakage to air). The considerable difference between leakage to air and leakage to soil indicates the importance of studying the soil effects on leakage discharge from pipes. As another matter of fact, it is obvious from Figure 5 that under the same pressures, the leakage in the coarser soil (Soil #1) is greater than in the finer soil (Soil #2). In all experiments, the leakage from Hole-3 is greater than that of the crack with an identical leak area, Crack-14.

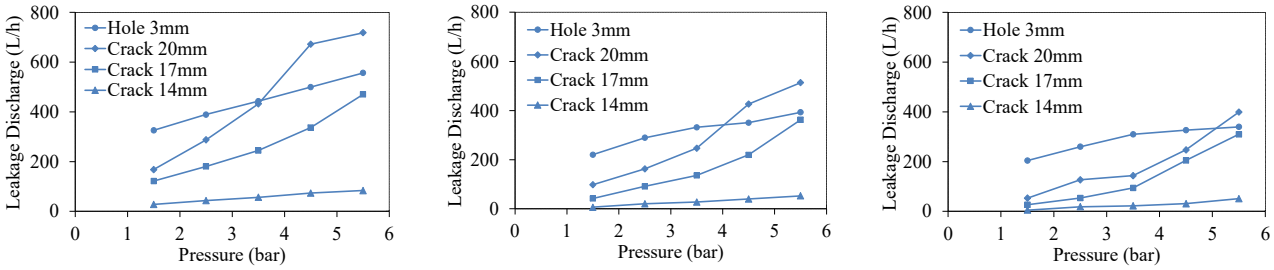

Figure 5. Leakage from various types of failure in pipes surrounded with (**a**) air, (**b**) Soil #1, and (**c**) Soil #2.

As shown in Figure 5, the impact of pressure and crack length varies between pipes surrounded by air and soil. Analysis of the leakage flow rate in Figure 5 led to the conclusion that three key factors affect the amounts of leakage flow rate: (1) the pressure inside the pipe, (2) the characteristics of the soils around the pipe, and (3) the dimensions of the failure.

The relationships between pressure and leakage discharge were obtained for various experiments, as given in Table 2, which are similar to Equation (2).

Table 2. The relationship between pressure and leakage discharge in different failures and surrounding conditions in this study.

Leakage Type	Equation		Surrounding Condition
Crack-14	$Q = 19.25P^{0.860}$	$R^2 = 0.998$	Free air
	$Q = 3.938P^{1.560}$	$R^2 = 0.973$	Soil #1
	$Q = 2.736P^{1.697}$	$R^2 = 0.946$	Soil #2
Crack-17	$Q = 75.14P^{1.015}$	$R^2 = 0.975$	Free air
	$Q = 21.04P^{1.595}$	$R^2 = 0.986$	Soil #1
	$Q = 10.53P^{1.914}$	$R^2 = 0.974$	Soil #2
Crack-20	$Q = 101.84P^{1.179}$	$R^2 = 0.987$	Free air
	$Q = 53.309P^{1.315}$	$R^2 = 0.979$	Soil #1
	$Q = 29.490P^{1.430}$	$R^2 = 0.954$	Soil #2
Hole-3	$Q = 271.34P^{0.408}$	$R^2 = 0.992$	Free air
	$Q = 189.25P^{0.430}$	$R^2 = 0.985$	Soil #1
	$Q = 177.55P^{0.403}$	$R^2 = 0.973$	Soil #2

Unlike the theoretical leakage–pressure relationship (Equation (2)) in which the leakage power equals 0.5, the present experimental studies for cracks yield values higher than

0.5. Table 2 shows that the value of leakage power for 14, 17 and 20 mm cracks is between 0.86 and 1.91. However, the value of the leakage exponent for the hole used in the present study was observed to be slightly less than 0.5, which may be due to the elasticity of the polyethylene material [14].

3.1. The Effect of Soil Surrounding the Pipe and Crack Length on the Leakage Discharge Coefficient

The values for leakage discharge coefficient (C) are presented in Table 3. The trends in Table 3 indicate that the leakage discharge coefficient increases by increasing the D_{50}, D_{10}, and C_u values of the soils. The discharge coefficient of the hole is significantly higher than the cracks, while it is higher in free air than in soils. Although [14] investigated the same results for uniform soils, this research confirms their conclusion for non-uniform soils.

Table 3. Calculated values of leakage discharge coefficient (C) in different failures and soils.

	Crack-14	Crack-17	Crack-20	Hole-3
Free air	19.25	75.14	101.84	271.34
Soil #1	3.938	21.04	53.309	189.25
Soil #2	2.736	10.53	29.490	177.55

Figure 6 shows variations in the leakage discharge coefficient in regard to the crack length. Increasing the crack length, the leakage coefficient increases. An increase in crack length from 14 to 20 mm increases the leakage coefficient between 5 and 13 times, depending on the surrounding conditions.

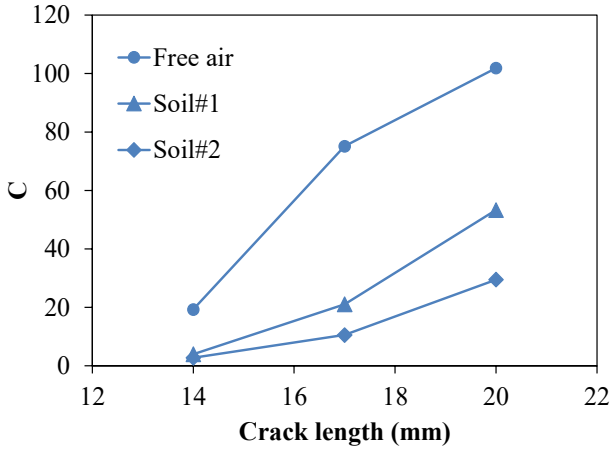

Figure 6. The relationship between leakage discharge coefficient and crack length.

As mentioned earlier, Crack-14 and Hole-3 are failures with different shapes but the same initial cross-sectional area. In order to provide a more comprehensive analysis and evaluation, the leakage discharges of Hole-3 are divided by those of Crack-14, in the corresponding pressures. As presented in Table 4, the results show that when the pressure increases, the ratios of hole/crack leakages decrease because the leakage opening size in the crack increases more rapidly than in the hole.

Table 4. Comparison of hole/crack leakage discharge for Hole-3 and Crack-14.

Pressure (bar)	Air	Soil #1	Soil #2
1.5	11.92	33.90	44.36
2.5	9.07	14.08	14.19
3.5	7.85	11.96	14.19
4.5	6.82	8.73	10.74
5.5	6.70	4.47	6.72

3.2. Characteristics of Fluidisation and Mobile Bed Zones

In this study, the experiments are performed using two types of non-uniform soils and four types of failure in the pipe at five different pressures. Once the water jet exits from the leak position, the fluid momentum overcomes the forces between soil particles and allows them to move freely. As a result, two zones, the fluidisation zone and the mobile bed zone, are formed. The zones gradually form throughout the test's run, and the experiments conclude once a steady state has been successfully achieved. Figures 7 and 8 indicate the shape of fluidisation and mobile bed zones at the steady state conditions in Soil #1 and Soil #2, respectively. The arrows represent the direction of soil/water flow.

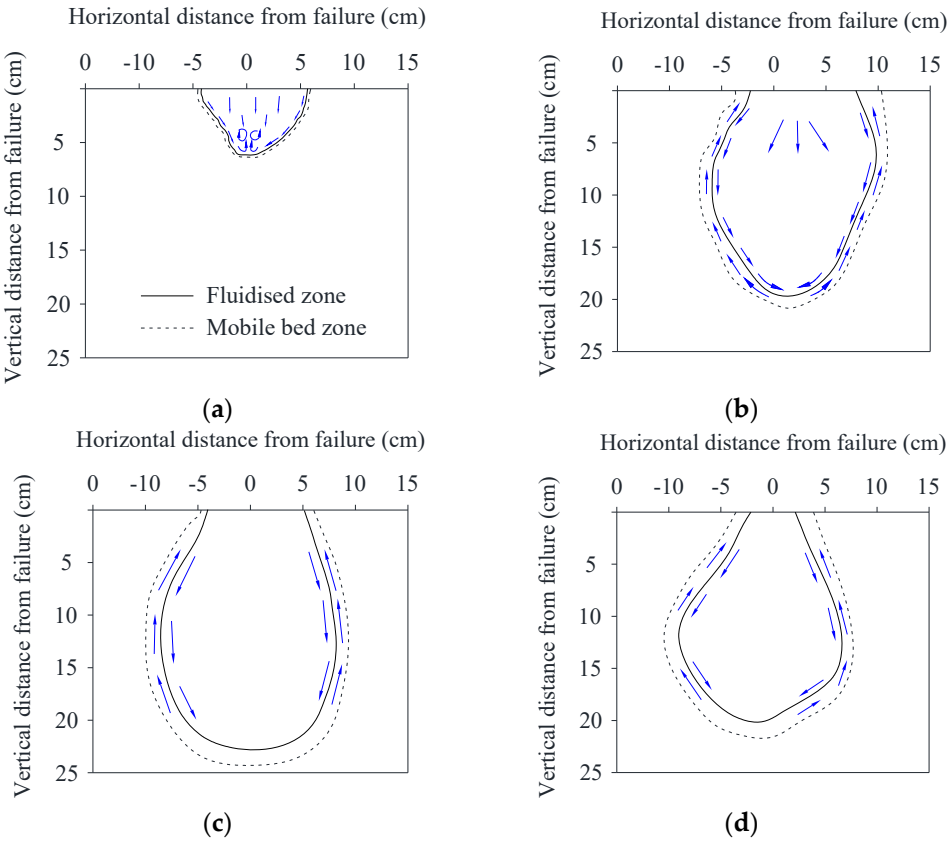

Figure 7. Fluidisation and mobile bed zones of Soil #1 in the steady state conditions at pressure 5.5 bar (maximum pressure) in (**a**) Crack-14; (**b**) Crack-17; (**c**) Crack-20; and (**d**) Hole-3.

Figure 9a,b shows variations in the height of the fluidisation zone with pressure in Soil #1 and Soil #2. It is clear that by increasing the pressure, the height of the fluidisation zone increases. By comparing the curves related to the orifice against the cracks' curves, it is indicated that the orifice has a lower slope than that of the cracks' curves, which is due to the different patterns of fluidisation development in the orifice and crack. Power regression was used to find empirical equations between the height of the fluidisation zone and the pressure in each failure and soil type, as presented in Table 5. For Soil #1, the exponent for Crack-14, Crack-17, Crack-20, and Hole-3 were obtained as 0.443, 1.341, 0.829, and 0.427, respectively. The corresponding exponents for Soil #2 are 0.514, 1.356, 1.384, and 0.427, respectively.

The changes in the height of the mobile bed zone with the pressure for the hole and different cracks are shown in Figure 9c,d, and the corresponding empirical equations are given in Table 5. For Soil #1, the exponents of the equations for Crack-17 and Crack-20 are close to 1, which indicates a near-linear pattern for these two curves. The mobile bed zone of Crack-14 was not developed for the pressures of 1.5 and 2.5 bar; therefore, the validity of the developed relationships for the pressure is in the range of 3.5 to 5.5 bar.

Also, considering the lower height changes in the mobile bed zone in the 14 mm crack in the mentioned interval, the amount of exponent in this relationship is lower than in other failures. In Soil #2, in all failure types, as the pressure increases, the height of the mobile bed zone increases (Figure 9d). According to Table 5, the changes in Crack-17 are almost linear (exponent close to 1). The exponent for Crack-20 is equal to 1.342, while for Crack-14 and Hole-3, the exponent is equal to 0.278 and 0.393, respectively, which indicates less sensitivity to the pressure in the latter failures compared to Crack-20 and Crack-17.

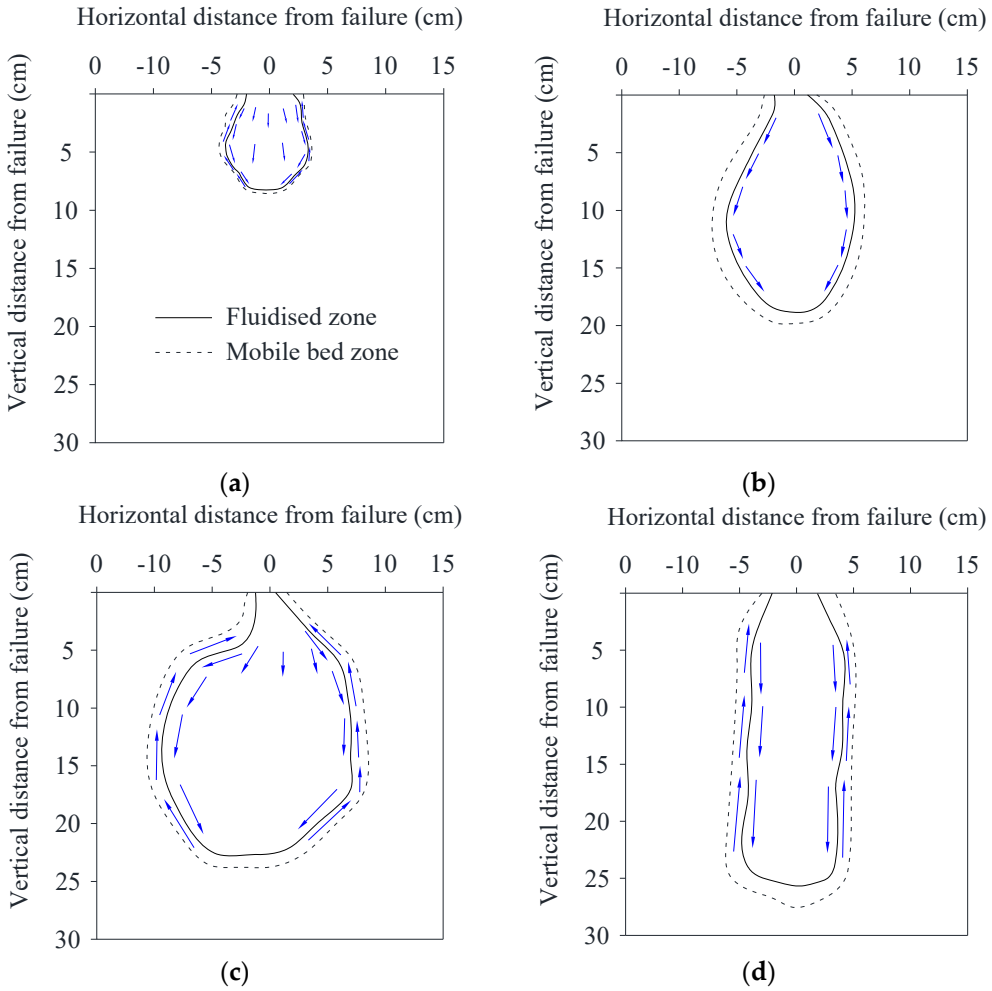

Figure 8. Fluidisation and mobile bed zones of Soil #2 at pressure 5.5 bar (maximum pressure) in (**a**) Crack-14; (**b**) Crack-17; (**c**) Crack-20; and (**d**) Hole-3.

Table 5. The regression equations for the height of the fluidisation zone and mobile bed zone in different failures and soils.

	Failure	Fluidisation Zone		Mobile Bed Zone	
Soil #1	Crack-14	$H_f = 3.1418P^{0.443}$	$R^2 = 0.933$	$H_m = 4.401P^{0.232}$, $3.5 \leq P \leq 5.5$	$R^2 = 0.676$
	Crack-17	$H_f = 2.162P^{1.341}$	$R^2 = 0.980$	$H_m = 2.347P^{1.315}$	$R^2 = 0.983$
	Crack-20	$H_f = 5.085P^{0.829}$	$R^2 = 0.869$	$H_m = 5.583P^{0.816}$	$R^2 = 0.880$
	Hole-3	$H_f = 9.202P^{0.427}$	$R^2 = 0.821$	$H_m = 9.481P^{0.475}$	$R^2 = 0.920$
Soil #2	Crack-14	$H_f = 3.292P^{0.514}$	$R^2 = 0.760$	$H_m = 5.190P^{0.278}$, $3.5 \leq P \leq 5.5$	$R^2 = 0.733$
	Crack-17	$H_f = 1.842P^{1.356}$	$R^2 = 0.990$	$H_m = 2.989P^{1.060}$, $2.5 \leq P \leq 5.5$	$R^2 = 0.951$
	Crack-20	$H_f = 2.289P^{1.384}$	$R^2 = 0.990$	$H_m = 2.593P^{1.342}$	$R^2 = 0.982$
	Hole-3	$H_f = 13.447P^{0.427}$	$R^2 = 0.993$	$H_m = 14.323P^{0.393}$	$R^2 = 0.996$

Notes: H_f is the height of the fluidisation zone and H_m is the height of the mobile bed zone.

The changes in the width of the fluidisation zone as a function of pressure for Soil #1 and Soil #2 are shown in Figure 10a,b. Generally, with increasing pressure, the value of the fluidisation width increases. In Soil #1, with Crack-14 and at lower pressures, usually due to the inability of the jet to move in the vertical direction, horizontal expansion of the fluidisation zone occurs more than vertical expansion, which is why, according to Figure 10a, the width of the fluidisation zone in Crack-14 under 1.5 bar pressure is the highest. Table 5 shows the regression equations obtained for fluidisation and mobile bed zone widths as a function of pressure. In this table, the exponent of the width–pressure relationship for Hole-3 in Soil #2 is equal to 0.221, which shows that the development of the fluidisation zone in the horizontal direction is limited in the hole.

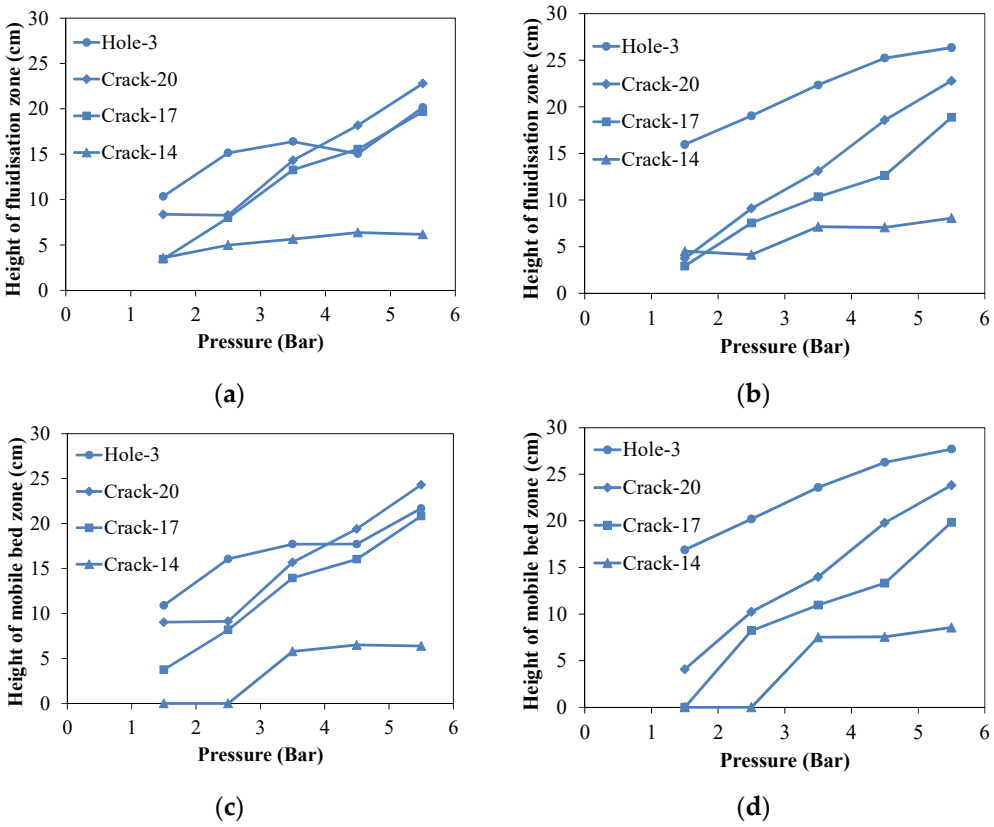

Figure 9. Height of the fluidisation zone and mobile bed zone in Soil #1 (**a**,**c**) and Soil #2 (**b**,**d**).

The changes in the width of the mobile bed zone in terms of pressure are shown in Figure 10c,d. The general increase in width as pressure increases is evident in this figure. Based on Figure 10c,d, experimental equations were also obtained for the width of the mobile bed (Table 6). According to Table 6, for Soil #1, the exponent of the width–pressure relationship for Crack-14, Crack-17, Crack-20, and Hole-3 are 0.678, 0.553, 0.651, and 0.628, respectively. For Soil #2, the width of Hole-3 changes very slightly at all pressures. The estimated exponent for Hole-3 in Soil #2 is 0.230 (Table 6), which indicates the limited horizontal development of the mobile bed in this case.

A shorter crack length and lower pressure can affect the water jet's ability to move vertically. With a smaller crack length, the water is more restricted to horizontal movement. This can result in instances where the width of fluidisation and mobile bed zones is greater in shorter cracks, as illustrated in Figure 10. Additionally, this phenomenon occurred at lower pressures in a failure compared to higher pressures. Although at some points the width of leakage zones decreases with increasing pressure, the area of the leakage zone uniformly increases in all cases.

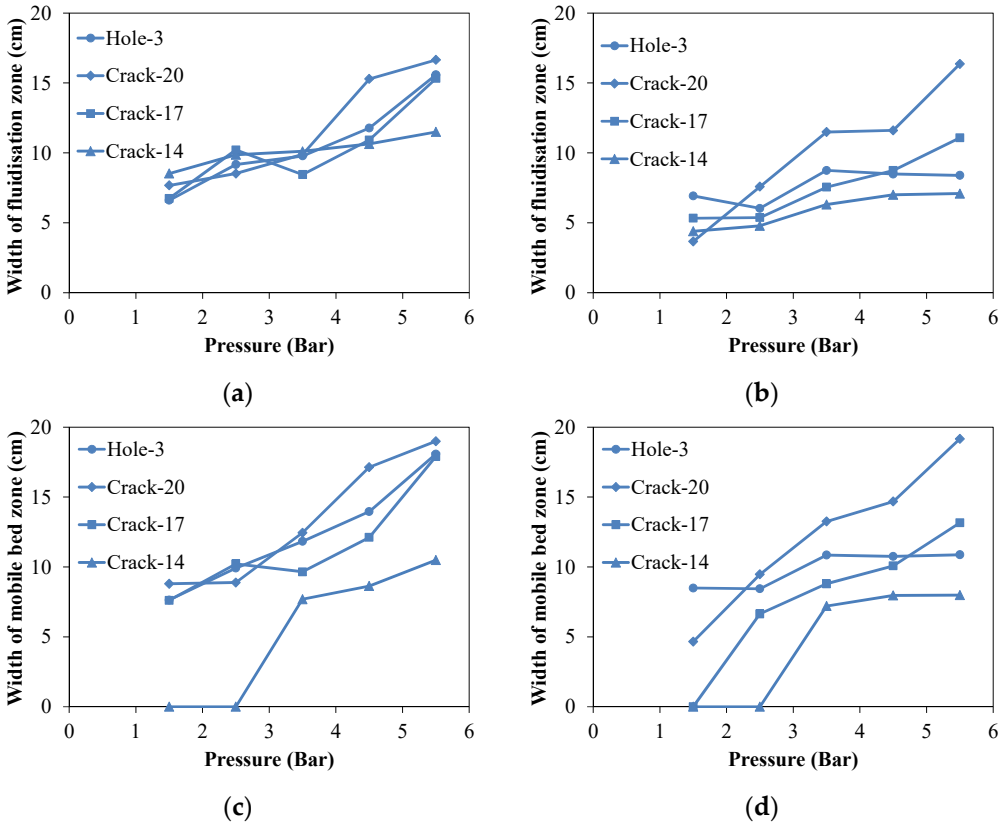

Figure 10. Width of the fluidisation zone and mobile bed zone in Soil #1 (**a**,**c**) and Soil #2 (**b**,**d**).

Table 6. The regression equations for the width of the fluidisation zone and mobile bed zone in different failures and soils.

	Failure	Fluidisation Zone		Mobile Bed Zone	
Soil #1	Crack-14	$W_f = 7.901P^{0.211}$	$R^2 = 0.961$	$W_m = 3.236P^{0.678}$, $3.5 \leq P \leq 5.5$	$R^2 = 0.956$
	Crack-17	$W_f = 5.496P^{0.513}$	$R^2 = 0.740$	$W_m = 5.810P^{0.553}$	$R^2 = 0.796$
	Crack-20	$W_f = 5.330P^{0.829}$	$R^2 = 0.860$	$W_m = 5.929P^{0.651}$	$R^2 = 0.866$
	Hole-3	$W_f = 5.090P^{0.630}$	$R^2 = 0.860$	$W_m = 5.689P^{0.628}$	$R^2 = 0.967$
Soil #2	Crack-14	$W_f = 3.579P^{0.418}$	$R^2 = 0.927$	$W_m = 5.435P^{0.235}$, $3.5 \leq P \leq 5.5$	$R^2 = 0.820$
	Crack-17	$W_f = 3.763P^{0.574}$	$R^2 = 0.989$	$W_m = 3.082P^{0.827}$, $3.5 \leq P \leq 5.5$	$R^2 = 0.997$
	Crack-20	$W_f = 2.537P^{1.099}$	$R^2 = 0.963$	$W_m = 3.280P^{1.050}$	$R^2 = 0.976$
	Hole-3	$W_f = 5.917P^{0.221}$	$R^2 = 0.492$	$W_m = 7.515P^{0.230}$	$R^2 = 0.767$

Notes: W_f is the width of the fluidisation zone and W_m is the width of the mobile bed zone.

The changes in the cross-sectional area of the fluidisation zone in terms of pressure are shown in Figure 11a,b for Soil #1 and Soil #2. According to this figure, it can be determined that with increasing pressure, the fluidisation area increases explicitly in all failure types. The empirical area–pressure equations of the fluidisation zone are presented in Table 7. As the exponents of these equations are quite close to 1 in Crack-14 and Hole-3, the changes can be considered almost linear. For Crack-17 and Crack-20, the exponents are 1.751 and 2.339, respectively.

The changes in the area of the mobile bed zone in terms of pressure for all failure types are shown in Figure 11c,d. Based on the obtained experimental equations (Table 7), the exponent for Crack-14, Crack-17, Crack-20, and Hole-3 for Soil #1 are 3.430, 2.018, 1.555, and 1.092, respectively, while the corresponding exponents for Crack-14, Crack-17, Crack-20, and Hole-3 for Soil #2 are equal to 0.541, 1.725, 2.372, and 0.768, respectively.

Considering the fluidisation equations in Table 6, the highest and the lowest exponents are for Crack-20 and Crack-14, respectively. In addition, the area–pressure exponent of

Hole-3 is close to 1, so the changes in the fluidisation area of the hole can be considered approximately linear. In addition, the mobile bed exponents for Crack-14, Crack-17, and Crack-20 are 3.430, nearly 2, and 1.555, respectively. Also, the variation in the mobile bed area is linear as well.

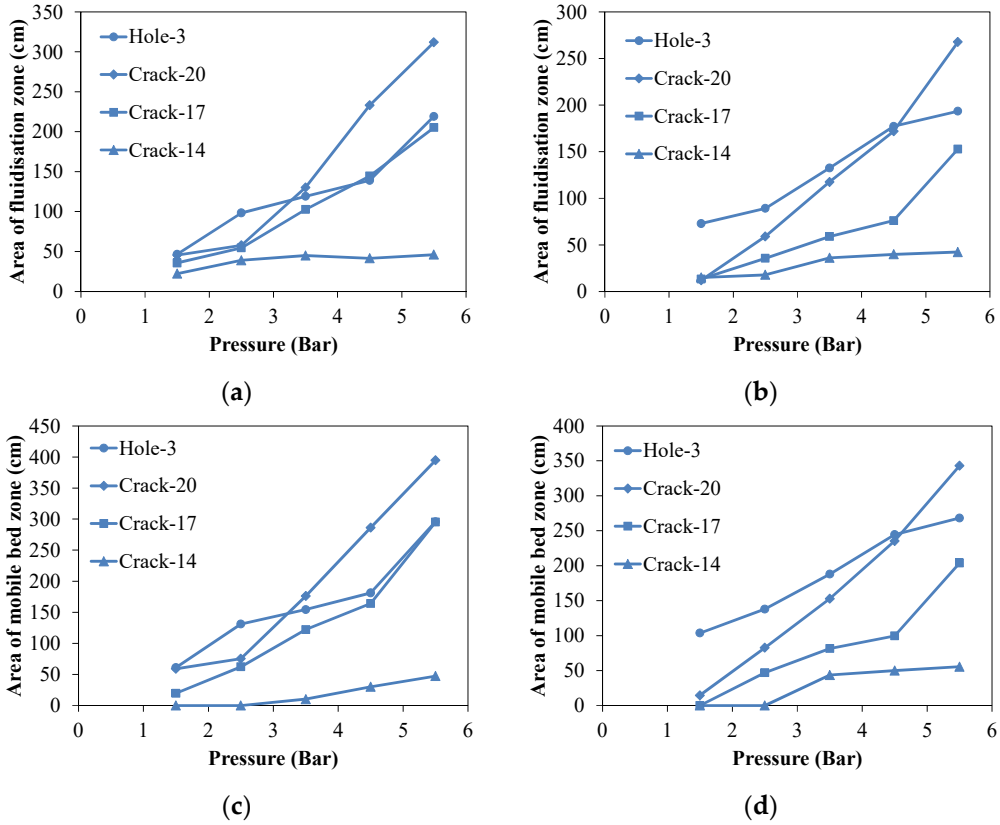

Figure 11. Cross-sectional area of fluidisation zone and mobile bed zone for Soil #1 (**a**,**c**) and Soil #2 (**b**,**d**).

Table 7. The regression equations for the area of fluidisation zone and mobile bed zone in different failures and soils.

	Failure	Fluidisation Zone		Mobile Bed Zone	
Soil #1	Crack-14	$A_f = 21.343P^{0.475}$	$R^2 = 0.961$	$A_m = 0.149P^{3.430}$, $3.5 \leq P \leq 5.5$	$R^2 = 0.908$
	Crack-17	$A_f = 18.480P^{1.370}$	$R^2 = 0.977$	$A_m = 9.079P^{2.018}$	$R^2 = 0.992$
	Crack-20	$A_f = 19.227P^{1.583}$	$R^2 = 0.930$	$A_m = 25.601P^{1.555}$	$R^2 = 0.936$
	Hole-3	$A_f = 31.609P^{1.083}$	$R^2 = 0.958$	$A_m = 41.270P^{1.092}$	$R^2 = 0.949$
Soil #2	Crack-14	$A_f = 9.462P^{0.944}$	$R^2 = 0.917$	$A_m = 22.133P^{0.541}$, $2.5 \leq P \leq 5.5$	$R^2 = 0.999$
	Crack-17	$A_f = 6.661P^{1.751}$	$R^2 = 0.980$	$A_m = 9.233P^{1.725}$, $3.5 \leq P \leq 5.5$	$R^2 = 0.934$
	Crack-20	$A_f = 5.518P^{2.339}$	$R^2 = 0.980$	$A_m = 6.878P^{2.372}$	$R^2 = 0.981$
	Hole-3	$A_f = 48.663P^{0.810}$	$R^2 = 0.958$	$A_m = 73.037P^{0.768}$	$R^2 = 0.985$

Notes: A_f is the width of the fluidisation zone and A_m is the width of the mobile bed zone.

As mentioned, Crack-14 and Hole-3 have the same initial leak area. Table 8 represents the values obtained by dividing the height, width, and area of the fluidisation zone of Hole-3 by their corresponding values for Crack-14. The values measured for all three cases in the two types of soils are almost equal with increasing pressure. Contrary to Table 4, the ratio of the hole-to-crack flow rate decreases with increasing pressure; for fluidisation, the changes are almost constant, which indicates that the change in the dimensions of the crack opening does not have much effect on the dimensions of the fluidisation area.

Table 8. Comparison of the ratios of the fluidisation zone dimensions of Hole-3 to those by Crack-14.

Pressure	Height of Fluidisation Zone		Width of Fluidisation Zone		Area of Fluidisation Zone	
	Soil #1	Soil #2	Soil #1	Soil #2	Soil #1	Soil #2
1.5	4.47	3.55	0.77	1.58	2.09	4.82
2.5	3.82	4.61	0.93	1.26	2.51	4.94
3.5	3.96	3.13	0.97	1.39	2.65	3.66
4.5	3.96	3.57	1.11	1.21	3.35	4.33
5.5	4.27	3.27	1.36	1.36	4.47	4.40

In the same way, Table 9 shows the ratios of the fluidisation zone dimensions due to Hole-3 to those of Crack-14 in terms of the height, width, and area of the mobile bed zones. In Table 8, the ratios are almost equal (except for the area of the mobile bed at the pressure of 3.5 bar), which indicates that the change in the dimensions of the crack opening does not have much effect on the dimensions of the mobile bed area. It should be noted that for Crack-14, the mobile bed area at the pressure of 1.5 and 2.5 bar was not formed; therefore, the ratio is not defined and denoted by N.D.

Table 9. Comparison of the ratios of the mobile bed zone dimensions of Hole-3 to those of Crack-14.

Pressure	Height of Mobile Bed Zone		Width of Mobile Bed Zone		Area of Mobile Bed Zone	
	Soil #1	Soil #2	Soil #1	Soil #2	Soil #1	Soil #2
1.5	N.D.	N.D.	N.D.	N.D.	N.D.	N.D.
2.5	N.D.	N.D.	N.D.	N.D.	N.D.	N.D.
3.5	3.06	3.13	1.53	1.51	15.11	4.31
4.5	2.72	3.47	1.61	1.35	6.0	4.88
5.5	3.39	3.23	1.72	1.36	6.24	4.83

Note: N.D. is Not Defined.

4. Conclusions

An experimental study has been conducted to assess the leakage and fluidisation around leaking water pipes buried in non-uniform soils. The fluidisation and mobile bed zones of soils were measured. Based on this study, the following is concluded:

1. A positive correlation exists between the height and area of the fluidisation/mobile bed zones and increasing pressure. The observed increase in the height ratio between the maximum and minimum pressure in different soils and failure scenarios indicates a range of 1.6 to 6.4 times for the fluidisation zone and 1.6 to 5.8 times for the mobile bed zone. Similarly, the area ratio between the maximum and minimum pressure exhibits an increase ranging from 2.1 to 22.3 times in the fluidisation zone and 2.6 to 23.6 times in the mobile bed zone, including diverse failures and soils of this study.
2. The pattern and trend of increasing the fluidisation zone and mobile bed zone in Crack-14 and Hole-3 (with the same initial cross-sectional area) are entirely different. By increasing the pressure, generally, the horizontal expansion of the fluidisation zone at the crack was more than the vertical one, while in the hole, with increasing pressure, the vertical expansion of the fluidisation and mobile bed zones was more than the horizontal one.
3. The patterns of developing leakage zones in Soil #1 and Soil #2 were also observed to be somewhat different from each other. Generally, in Soil #1, which is more coarse-grained, with increasing pressure, larger horizontal expansion was observed than vertical expansion. In contrast, in Soil #2, with increasing pressure, more significant vertical expansion was observed than horizontal expansion.
4. In all experiments conducted in an open-air environment, the observed leakage flow rate was greater than the leakage flow rate seen in soil (between 1.3 and 5.9 times increase observed in the results). This disparity can be attributed to the presence of soil particles surrounding the crack, which effectively hinder the water from exiting the pipe.

5. The coarsening of soil is associated with an increase in leakage; the ratio of leakage in soil with a coarser grain size (Soil #1) to soil with a finer grain size (Soil #2) shows an increase ranging from 1.1 to 1.9 times under equal pressure conditions.
6. The leakage flow rate in Hole-3 is significantly greater than that of the crack with the equivalent area (Crack-14). The results indicate an observable increase in leakage flow ranging from 1.3 to 5.9 times under equal pressure conditions.
7. The significance of the matter lies in the occurrence of fluidisation, which leads to soil loosening around the pipe, resulting in diminished support and eventual pipe failure. Therefore, this study serves as a valuable guide for engineers to be mindful of and mitigate issues arising from fluidisation.
8. To delve deeper into studying the phenomenon of fluidisation, exploring the influencing factors, its progression, and preventive measures, further research is warranted in the future. A critical aspect in this domain is understanding the correlation between the expansion of the fluidisation area and the likelihood of pipe failure in soils with varying characteristics. It is crucial to identify methods that can constrain the formation and growth of these areas as their expansion escalates the risk of pipe failure.

Author Contributions: Conceptualization, M.L.; methodology, S.S., M.L. and M.G.; validation, S.S. and M.L.; formal analysis, S.S.; investigation, S.S.; resources, S.S.; data curation, M.L.; writing—original draft preparation, S.S.; writing—review and editing, M.L. and M.G.; visualization, M.L.; supervision, M.L. and M.G. All authors have read and agreed to the published version of the manuscript.

Funding: This research received no external funding.

Data Availability Statement: Some or all of the data, models, or code that support the findings of this study are available from the corresponding author upon reasonable request.

Acknowledgments: The authors are genuinely grateful to the University of Exeter for covering the APC.

Conflicts of Interest: The authors declare no conflicts of interest.

References

1. Van Zyl, J.E.; Clayton, C.R.I. The effect of pressure on leakage in water distribution systems. *Water Manag.* **2007**, *160*, 109–114. [CrossRef]
2. The World Bank. The World Bank and the International Water Association to Establish a Partnership to Reduce Water Losses. 2016. Available online: https://www.worldbank.org/en/news/press-release/2016/09/01/the-world-bank-and-the-international-water-association-to-establish-a-partnership-to-reduce-water-losses (accessed on 1 February 2024).
3. Liemberger, R.; Wyatt, A. Quantifying the global non-revenue water problem. *Water Sci. Technol. Water Supply* **2018**, *19*, 831–837. [CrossRef]
4. De Jesús Mora Rodríguez, J.; Delgado-Galván, X.; Ramos, H.M.; Jiménez, P.A.L. An overview of leaks and intrusion for different pipe materials and failures. *Urban Water J.* **2013**, *11*, 1–10. [CrossRef]
5. Van Zyl, J.E.; Alsaydalani, M.O.A.; Clayton, C.R.I.; Bird, T.; Dennis, A. Soil fluidisation outside leaks in water distribution pipes—Preliminary observations. *Water Manag.* **2013**, *166*, 546–555. [CrossRef]
6. Giustolisi, O.; Savić, D.; Kapelan, Z. Pressure-Driven demand and leakage simulation for water distribution networks. *J. Hydraul. Eng.* **2008**, *134*, 626–635. [CrossRef]
7. Walski, T.M.; Bezts, W.; Posluszny, E.T.; Weir, M.; Whitman, B. Modeling leakage reduction through pressure control. *J. AWWA* **2006**, *98*, 147–155. [CrossRef]
8. Cordell, D.; Drangert, J.-O.; White, S.W. The story of phosphorus: Global food security and food for thought. *Glob. Environ. Chang.* **2009**, *19*, 292–305. [CrossRef]
9. Cassa, A.M.; Van Zyl, J.E.; Laubscher, R.F. A numerical investigation into the effect of pressure on holes and cracks in water supply pipes. *Urban Water J.* **2010**, *7*, 109–120. [CrossRef]
10. Greyvenstein, B.; Van Zyl, J.E. An experimental investigation into the pressure-leakage relationship of some failed water pipes. *Aqua* **2007**, *56*, 117–124. [CrossRef]
11. Farley, M.; Trow, S. Losses in Water Distribution Networks: A Practitioners' Guide to Assessment, Monitoring and control. *Water Intell. Online* **2015**, *4*, 9781780402642. [CrossRef]
12. Sadr-Al-Sadati, S.A.; Ghazizadeh, M.J. The experimental and numerical study of water leakage from High-Density Polyethylene pipes at elevated temperatures. *Polym. Test.* **2019**, *74*, 274–280. [CrossRef]

13. Zhai, Q.; Ye, W.; Rahardjo, H.; Satyanaga, A.; Du, Y.-J.; Dai, G.; Zhao, X. Estimation of the hydraulic conductivity of unsaturated soil incorporating the film flow. *Can. Geotech. J.* **2022**, *59*, 1679–1684. [CrossRef]
14. Latifi, M.; Naeeni, S.T.; Mahdavi, A. Experimental assessment of soil effects on the leakage discharge from polyethylene pipes. *Water Supply* **2017**, *18*, 539–554. [CrossRef]
15. Latifi, M.; Parvaneh, R.; Naeeni, S.T.O. Investigating the influence of surrounding soil properties on leakage discharge from cracks in polyethylene pipes. *Eng. Fail. Anal.* **2022**, *141*, 106676. [CrossRef]
16. Alsaydalani, M.O.A.; Clayton, C.R.I. Internal fluidization in granular soils. *J. Geotech. Geoenviron. Eng.* **2014**, *140*, 04013024. [CrossRef]
17. Latifi, M.; Mohammadbeigi, S.; Moghadam, K.F.; Naeeni, S.T.O.; Kilanehei, F. Experimental study of pressure and soil effects on fluidization and mobile bed zones around buried leaking pipes. *J. Pipeline Syst. Eng. Pract.* **2022**, *13*, 04022034. [CrossRef]
18. Bailey, N.D.; Van Zyl, J.E. Experimental investigation of internal fluidisation due to a vertical water leak jet in a uniform medium. *Procedia Eng.* **2015**, *119*, 111–119. [CrossRef]
19. Pike, S.; Van Zyl, J.E.; Clayton, C.R.I. Scouring damage to buried pipes caused by leakage jets: Experimental study. *J. Pipeline Syst. Eng. Pract.* **2018**, *9*, 04018020. [CrossRef]
20. Nguyên, T.T.; Indraratna, B. A Coupled CFD–DEM Approach to Examine the Hydraulic Critical State of Soil under Increasing Hydraulic Gradient. *Int. J. Geomech.* **2020**, *20*, 04020138. [CrossRef]
21. Alsaydalani, M.O.A. Effect of orifice hydraulic and geometric characteristics on leakage in water distribution systems. *Int. J. GEOMATE Geotech. Constr. Mater. Environ.* **2023**, *25*, 59–67. [CrossRef]
22. Monzer, A.; Faramarzi, A.; Yerro, A.; Chapman, D. MPM investigation of the fluidization initiation and postfluidization mechanism around a pressurized leaking pipe. *J. Geotech. Geoenviron. Eng.* **2023**, *149*, 04023096. [CrossRef]
23. Akrami, S.; Bezuijen, A.; Van Beek, V.; Terwindt, J. The effect of relative density on the response of sand to internal fluidization. *Acta Geotech.* **2022**, *18*, 319–333. [CrossRef]
24. Nguyên, T.T.; Indraratna, B. Fluidization of soil under increasing seepage flow: An energy perspective through CFD-DEM coupling. *Granul. Matter* **2022**, *24*, 80. [CrossRef]
25. Das, B.M. *Principles of Geotechnical Engineering*, 10th ed.; Cengage Learning: Boston, MA, USA, 2022.
26. *ASTM D2487-17*; Standard Practice for Classification of Soils for Engineering Purposes (Unified Soil Classification System). American Society for Testing and Materials (ASTM): West Conshohocken, PA, USA, 2017. [CrossRef]
27. *ASTM D698-12*; Standard Test Methods for Laboratory Compaction Characteristics of Soil Using Standard Effort (12,400 ft-lbf/ft^3 (600 kN-m/m^3)). American Society for Testing and Materials (ASTM): West Conshohocken, PA, USA, 2021. [CrossRef]